Nationaal Lucht- en Ruimtevaartlaboratorium

National Aerospace Laboratory NLR

NLR-TP-2013-218

Azimuthal and radial mode detection by a slowly rotating rake in an aircraft turbofan engine

AIAA Paper 2013-2244

P. Sijtsma and H. Orsi

Nationaal Lucht- en Ruimtevaartlaboratorium
National Aerospace Laboratory NLR

Anthony Fokkerweg 2
P.O. Box 90502
1006 BM Amsterdam
The Netherlands
Telephone +31 (0)88 511 31 13
Fax +31 (0)88 511 32 10
Web site: http://www.nlr.nl

Nationaal Lucht- en Ruimtevaartlaboratorium

National Aerospace Laboratory NLR

Executive summary

Azimuthal and radial mode detection by a slowly rotating rake in an aircraft turbofan engine

AIAA Paper 2013-2244

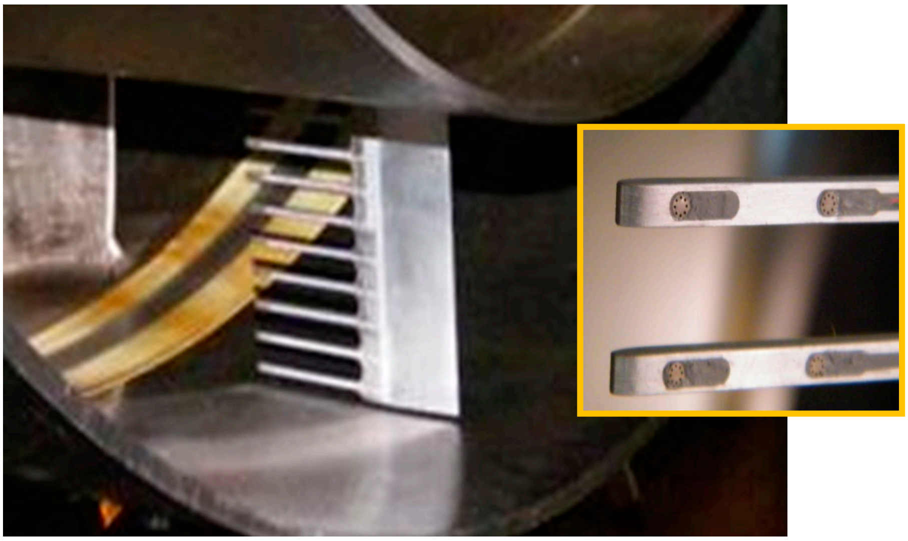

Report no.
NLR-TP-2013-218

Author(s)
P. Sijtsma
H. Orsi

Report classification
UNCLASSIFIED

Date
May 2013

Knowledge area(s)
Aëro-akoestisch en experimenteel aërodynamisch onderzoek

Descriptor(s)
Mode detection
Radial modes
Annular duct

Problem area
The Low Pressure Turbine (LPT) of an aircraft turbofan engine can contribute significantly to the total engine noise, especially during approach. LPT noise is caused by interaction between rotors and stators in the various turbine stages, and is usually dominated by Blade Passing Frequency tones.

It is very useful to have a detailed description of the acoustic field in the flow duct downstream of the LPT, in terms of azimuthal and radial duct modes. Herewith, the following information can be retrieved:

- assessment of the noisiest turbine stage,
- distinction between upstream and downstream noise propagation,
- determination of the acoustic intensity,
- estimation of far-field sound radiation.

Duct modes can be measured by means of radial rakes instrumented with pressure transducers or a rotating axial transducer array mounted flush in the duct wall.

Description of work
This paper presents a new detection method for azimuthal and radial acoustic modes in a cylindrical flow duct. It features a radial rake which performs one full rotation through the duct, in a slow continuous

This report is based on a presentation held at the 19th AIAA/CEAS Aeroacoustics Conference, Berlin, Germany, May 27-29, 2013.

motion. The typical rotation time is 10 minutes.

Results and conclusions
The measurement time of 10 minutes is significantly shorter than with conventional radial mode detection methods, where measurements are done at a large number of static rake positions. On the other hand, the rake rotation speed is much lower than the shaft speed, so that time-consuming corrections for Doppler frequency shift are not needed. As a result, the post-processing time is relatively short, say 10 minutes also. Thus, the advantages of a short acquisition time and a short processing time are combined. The merits of the new mode detection device are discussed by means of an error analysis.

Applicability
In this paper, applications are shown to typical measurements on an LPT component. The mode detection method can also be applied to measurements in the intake or the bypass duct of a turbofan engine

Nationaal Lucht- en Ruimtevaartlaboratorium, National Aerospace Laboratory NLR

Anthony Fokkerweg 2, 1059 CM Amsterdam,
P.O. Box 90502, 1006 BM Amsterdam, The Netherlands
Telephone +31 88 511 31 13, Fax +31 88 511 32 10, Web site: www.nlr.nl

Nationaal Lucht- en Ruimtevaartlaboratorium

National Aerospace Laboratory NLR

NLR-TP-2013-218

Azimuthal and radial mode detection by a slowly rotating rake in an aircraft turbofan engine

AIAA Paper 2013-2244

P. Sijtsma and H. Orsi[1]

[1] Snecma (Safran Group)

This report is based on a presentation held at the 19th AIAA/CEAS Aeroacoustics Conference, Berlin, Germany, May 27-29, 2013.

This publication has been refereed by the Advisory Committee AEROSPACE VEHICLES.

Customer	Snecma (Safran Group)
Contract number	920 457853
Owner	NLR
Division NLR	Aerospace Vehicles
Distribution	Unlimited
Classification of title	Unclassified
	May 2013

Approved by:

Author	Reviewer	Managing department
P. Sijtsma	M. Oppeneer	J. Hakkaart
Date: 15-05-13	Date: 16-5-13	Date: 17-5-'13

Contents

Azimuthal and radial mode detection by a slowly rotating rake in an aircraft turbofan engine

Pieter Sijtsma*
National Aerospace Laboratory NLR, 8300 AD Emmeloord, The Netherlands

Hélène Orsi†
Snecma Villaroche, SAFRAN Group, 77550 Moissy-Cramayel, France

This paper presents a new detection device for azimuthal and radial acoustic modes in a cylindrical flow duct. It features a radial rake, instrumented with pressure transducers, which performs one full rotation through the duct, in a slow continuous motion. The typical rotation time is 10 minutes. This is significantly shorter than with conventional radial mode detection methods, where measurements are done at a large number of static rake positions. On the other hand, the rake rotation speed is much lower than the shaft speed, so that time-consuming corrections for Doppler frequency shift are not needed. As a result, the post-processing time is relatively short, say 10 minutes also. Thus, the advantages of a short acquisition time and a short processing time are combined. The merits of the new mode detection device are discussed by means of an error analysis. Applications are shown to typical measurements on a Low Pressure Turbine component.

Nomenclature

BPF	=	Blade Passing Frequency
LPT	=	Low Pressure Turbine
TRF	=	Turbine Rear Frame
$A^{\pm}_{m\mu}$	=	mode amplitude (upstream/downstream)
$A^{\pm}_{m\mu,n}$	=	mode amplitude, Eq. (20)
$a_{m\mu,n}$	=	amplitude of radial mode, Eq. (19)
b_m	=	amplitude of azimuthal mode
$b_{m,n,k}$	=	amplitude of azimuthal mode, Eq. (18)
c_0	=	sound speed (m/s)
$E\{\ \}$	=	expectation value
f	=	frequency (Hz)
f_{sam}	=	sample frequency (Hz)
$G_{m\mu}$	=	radial eigenfunction
h	=	hub to tip ratio
i	=	imaginary unit
J	=	number of shaft revolutions
J_m	=	m-th order Bessel-function
j	=	shaft revolution index
K	=	number of radial sensor positions
k	=	sensor index
l	=	sample index
$l_{\max}$	=	number of samples in interval $t_j \le \tau \le t_{j+1}$
M	=	Mach number of axial flow
m	=	azimuthal order
m_0	=	input azimuthal order
N	=	maximum engine order
n	=	engine order
n_0	=	input engine order
p	=	acoustic pressure
$p_{n,k,j}$	=	complex pressure amplitude, Eq. (16)
$Q_{m\mu,n}$	=	See Eq. (25)
R_{inner}	=	inner duct radius (m)
R_{outer}	=	outer duct radius (m)
r	=	radial coordinate
r_k	=	radial sensor location
$s_k(t)$	=	pressure signal
$s_{k,l}$	=	sampled pressure, Eq. (15)
t	=	time
t_j	=	pulse time
U	=	speed of uniform axial flow (m/s)
x	=	axial coordinate
x_1, x_2	=	axial locations of sensors
Y_m	=	m-th order Neumann-function
$\alpha^{\pm}_{m\mu}$	=	axial eigenvalue
$\alpha^{\pm}_{m\mu,n}$	=	axial eigenvalue, Eq. (21)
β^2	=	$1-M^2$

* Senior Scientist, Department of Helicopters & Aeroacoustics, P.O. Box 153.
† Research Engineer, Acoustics Department, Snecma.

Δx	=	axial distance between sensors	σ	=	standard deviation of rake position
δ_j	=	rake position error	τ_l	=	sample time
$\varepsilon_{m\mu}$	=	radial eigenvalue	$\xi_{m\mu}(\omega)$	=	see Eq. (9)
γ_j	=	pulse time error	Ω	=	angular shaft speed
μ	=	radial order (starting with $\mu = 1$)	Ω_a	=	assumed angular shaft speed
θ	=	azimuthal angle	ω	=	angular frequency
θ_1, θ_2	=	azimuthal bounds of rake motion	ω_n	=	angular frequency of n-th engine order
θ_j	=	angular rake position	ψ	=	angular speed of the rake
ρ_0	=	air density (kg/m^3)			

I. Introduction

THE Low Pressure Turbine (LPT) of an aircraft turbofan engine can contribute significantly to the total engine noise, especially during approach[1,2]. LPT noise is caused by interaction between rotors and stators in the various turbine stages (rotor-stator combinations), and is usually dominated by Blade Passing Frequency (BPF) tones.

In order to trace the dominant noise source mechanisms, it is very useful to have detailed information about the acoustic field in the flow duct downstream of the LPT. Basic information can be obtained by making a decomposition of the sound field into azimuthal (circumferential) modes, using wall-mounted circular arrays of transducers[3]. Comparison of measured dominant modes with expected modes[4] from the various rotor-stator combinations gives information about the stages that give the most important contributions.

Full information about the sound field is obtained by decomposing the azimuthal modes further into radial duct modes. This offers the following additional benefits:

- Distinction can be made between upstream and downstream propagation.
- The acoustic intensity can be determined.
- The radial mode decomposition can be used as input to calculations of far-field sound radiation.

Radial (and thus azimuthal) duct modes can be measured by means of radial rakes instrumented with pressure transducers[5-7] or by means of a rotating axial transducer array mounted flush in the duct wall[6].

The most straightforward way to determine duct modes from the above-mentioned devices is to acquire data from several angular transducer positions, while correlating with a shaft trigger signal. As the number of angular positions needs to be larger than twice the largest propagating azimuthal mode number, the data acquisition may be a time consuming process, requiring a long test bench occupation time.

A mode detection system based on a continuously rotating rake was developed by NASA[7,8]. The rake rotation speed was coupled to the shaft speed. With such a device data acquisition can be done in a short time. However, a disadvantage is the occurrence of Doppler frequency shift, dependent on mode number, which strongly affects the post-processing time.

This paper presents a new mode detection device based on a *slowly* rotating rake. Typically, 10 minutes are used for a full rake rotation. Herewith, the time needed to traverse between many static positions is saved, thus making the measurements cheaper and less complicated. On the other hand, the rake rotation speed is much lower than the shaft speed, which means that effects of Doppler frequency shift can be neglected. As a result, the post-processing time is relatively short, say 10 minutes also. Hence, this device combines the advantages of a short acquisition time and a short processing time.

The concept of a slowly rotating rake was applied to measurements on an LPT component in Snecma's "1T" test facility. The rake consisted of 10 holders, each instrumented with 2 pressure transducers (see Figure 1). It was mounted on the inner sleeve of the annular duct downstream of the LPT component.

In Section II of this paper a review is given of the modal representation of the sound field. Section III gives a brief description of the test set-up. In Section IV the mode detection method is explained. Section V gives an error analysis. The merits of the method are demonstrated by some typical examples in Section VI.

II. Representation of sound field in duct modes

A. Basic assumptions

We consider sound propagation in an annular duct, of which the geometry does not change in axial direction. Using cylindrical coordinates (x, r, θ), the duct is described by

$$\{(x,r,\theta);\ R_{\text{inner}} \le r \le R_{\text{outer}}\}\ . \tag{1}$$

In the duct, a uniform subsonic flow U is assumed in the positive x-direction. All physical quantities are made dimensionless on outer duct radius R_{outer}, air density ρ_0 and sound speed c_0. The Mach number of the axial flow is

$$M = U/c_0\ . \tag{2}$$

The dimensionless geometry is described by

$$\{(x,r,\theta);\ h \le r \le 1\}\ , \tag{3}$$

in which the hub/tip ratio h is defined by

$$h = R_{\text{inner}}/R_{\text{outer}}\ . \tag{4}$$

The relation between the dimensionless angular frequency (Helmholtz number) ω and the physical frequency f is

$$\omega = 2\pi f R_{\text{outer}}/c_0\ . \tag{5}$$

For frequency-domain expressions the $\exp(+i\omega t)$ convention is used.

B. Expression in modes

At fixed frequency (ω) the acoustic pressure field in an annular duct can be expressed by a summation of modes:

$$p(x,r,\theta) = \sum_{m=-\infty}^{\infty} b_m(x,r)e^{-im\theta} = \sum_{m=-\infty}^{\infty}\left\{\sum_{\mu=1}^{\infty}\left(A^+_{m\mu}e^{i\alpha^+_{m\mu}x} + A^-_{m\mu}e^{i\alpha^-_{m\mu}x}\right)G_{m\mu}(r)\right\}e^{-im\theta}\ . \tag{6}$$

If the duct is not acoustically treated, the radial eigenfunctions $G_{m\mu}(r),\ \mu = 1,2,...$ form orthogonal sets. The axial eigenvalues $\alpha^{\pm}_{m\mu}$ are given by

$$\begin{cases}\alpha^+_{m\mu} = \left(M\omega - \xi_{m\mu}(\omega)\right)/\beta^2\ ,\\ \alpha^-_{m\mu} = \left(M\omega + \xi_{m\mu}(\omega)\right)/\beta^2,\end{cases} \tag{7}$$

with

$$\beta^2 = 1 - M^2\ , \tag{8}$$

$$\begin{cases}\xi_{m\mu}(\omega) = \omega\sqrt{1-\left(\varepsilon_{m\mu}\beta/\omega\right)^2}\ ,\ \text{for } \left(\varepsilon_{m\mu}\beta\right)^2 < \omega^2,\\ \xi_{m\mu}(\omega) = -i\sqrt{\left(\varepsilon_{m\mu}\beta\right)^2 - \omega^2}\ ,\ \text{for } \left(\varepsilon_{m\mu}\beta\right)^2 \ge \omega^2.\end{cases} \tag{9}$$

In Eq. (9), $\varepsilon_{m\mu}$ are radial eigenvalues, which are the solutions of

$$J_m(\varepsilon_{m\mu})Y'_m(\varepsilon_{m\mu}h) - Y_m(\varepsilon_{m\mu})J'_m(\varepsilon_{m\mu}h) = 0\ . \tag{10}$$

Herein J_m and Y_m are the m-th order Bessel and Neumann functions, respectively.

III. Experimental set-up

A. Facility

Tests on an LPT component, consisting of a number of rotor/stator stages, were carried out in Snecma's "1T" test facility in Villaroche, France. The LPT component is a scaled model of a representative "state-of-the-art" multi-stages LPT. The test bench includes gas boost and extractor compressors, an LPT component with water brake, and an auxiliary compressor. The boost compressor feeds the LPT with air compressed at 3 bars, fixed temperature close to 200 °C, and a mass flow up to around 16 kg/s at design point. Depending on targeted operating point pressure ratio, the LPT is controlled in such manner that the exit can be coupled either to the extractor (in the case of depression) or to the ambient conditions. LPT water brake situated on the LPT shroud line allows absorption of extracted power from the turbine, therefore regulating the speed with water flow alimentation variations. Boost and extraction compressors are mechanically driven by electrical engines of 7.5 MW power. The auxiliary gas compressor feeds the network in 15 bars compressed air used for ventilation circuits and purge, as well as pressurization needed to prevent the axial thrust of the machine.

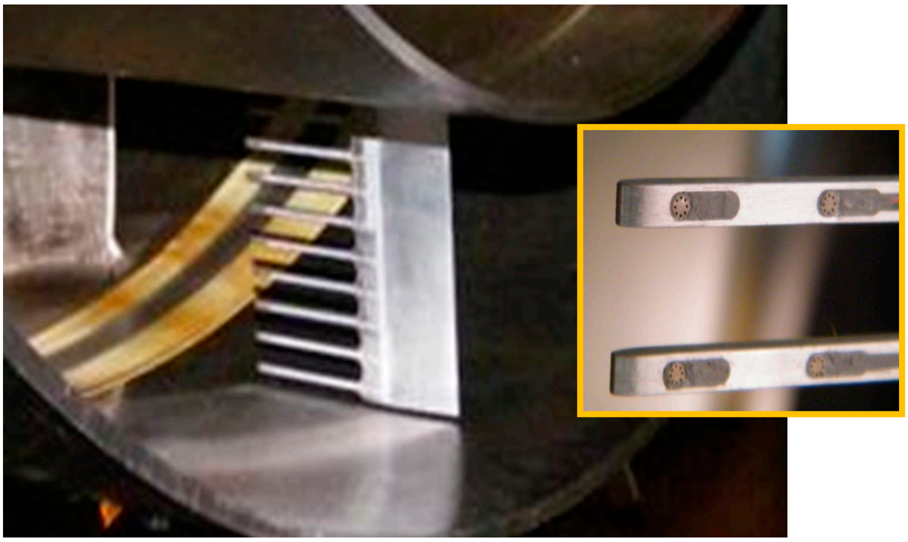

Figure 1 Rotating rake, with close-up of Kulite sensor holders.

B. Rotating rake

To measure the duct modes, a rake was mounted in the straight annular section downstream of the LPT component. The hub/tip ratio of this part of the duct is approximately $h = 0.7$. The duct was not treated with acoustical liners.

The rake consists of $K = 10$ holders, located at

$$r_k = h + (1-h)(k-0.5)/K, \quad k = 1,\ldots,K . \tag{11}$$

Each rake holder is instrumented with 2 Kulite sensors at the following axial locations:

$$\begin{cases} x_1 = 0, \\ x_2 = \Delta x = 0.034 \end{cases} \tag{12}$$

The rake was mounted on the inner sleeve (see Figure 1), which is able to make an almost full rotation. Less than 4° could not be covered. The axial location of the rake was more than 1.5 chords away from the "Turbine Rear Frame" (TRF) exit guide vanes, in order to minimize wake interaction effects.

For most measurements 10 minutes were used to make a full rotation, which is significantly shorter than conventional measurements with many static angular rake positions. The shaft speed varied between a number of typical approach speed conditions of a modern aircraft engine LPT. Unlike NASA's rotating rake device[7,8], the rake rotation is much slower than the shaft rotation.

In order to track the position of the rake, a slowly varying DC-signal was recorded simultaneously with the acoustic data. The shaft position was tracked by means of a 1/rev pulse signal.

C. Range of propagating modes

It follows from Eq. (9) that a duct mode is propagating when the corresponding radial eigenvalue satisfies the following condition:

$$\varepsilon_{m\mu} < \omega/\beta . \tag{13}$$

For the tests under consideration, mode detection is required at dimensionless frequencies ω with $\omega/\beta \le 99$ (which includes the BPF tones of the rotors). Hence, we need to detect modes with eigenvalues up to 99. These eigenvalues are obtained for azimuthal orders in the range $-95 \le m \le +95$ and for radial orders up to $\mu = 9$.

IV. Mode detection method

A. Engine order Fourier transforms

First, the pulse times t_j are determined. This is a series of times that correspond with a fixed shaft position. The pulse times can be obtained from the 1/rev pulse signal. When the pulse times are known, the shaft speed and the relative shaft angles can be calculated at any point in time.

Then, a Fourier transform can be performed for each sensor and in each time interval $t_j \le t \le t_{j+1}$ between two pulses:

$$p_{k,j,n} = \frac{2}{t_{j+1} - t_j} \int_{t_j}^{t_{j+1}} s_k(t) \exp\left(-2\pi i n \frac{t - t_j}{t_{j+1} - t_j} \right) dt \,, \tag{14}$$

where $s_k(t)$ is the pressure signal from sensor *k*. Thus, complex spectra $p_{k,j,n}$, $n = 1,...,N$, are calculated, where *n* is the engine order (or shaft order). The time signals $s_k(t)$ are sampled at a fixed sample frequency f_{sam}:

$$s_k(\tau_l) = s_{k,l} \,, \;\; \tau_{l+1} - \tau_l = 1/f_{\text{sam}} \,. \tag{15}$$

Therefore, we can evaluate Eq. (14) as

$$p_{n,k,j} = \frac{2}{l_{\max}} \sum_{l=1}^{l_{\max}} s_{k,l} \exp\left(-2\pi i n \frac{\tau_l - t_j}{t_{j+1} - t_j} \right), \tag{16}$$

where $t_j \le \tau_1 < \tau_2 < .... < \tau_{l_{\max}} < t_{j+1}$. Since the number $l_{\max}$ of samples in an interval $t_j \le \tau \le t_{j+1}$ is in general not a power of 2, an FFT is not possible. The discrete Fourier transform is therefore directly evaluated with Eq. (16).

The number $l_{\max}$ determines the relevant range of engine orders. To avoid aliasing, the maximum engine order *N* has to satisfy:

$$N < l_{\max}/2 \,. \tag{17}$$

If *N* is set too high, then the results at the highest engine orders are aliased results from lower engine orders. The engine order $n = l_{\max}/2$ corresponds with the Nyquist frequency in conventional signal processing. Noise at higher engine orders has to be sufficiently low (or filtered out) in order to avoid aliasing from high to low frequencies. This is guaranteed by the use of an anti-aliasing filter during acquisition.

B. Determination of azimuthal and radial modes

Amplitudes of azimuthal modes are calculated by averaging. For each shaft revolution *j*, we update the azimuthal mode spectrum according to

$$b_{m,n,k} = \left((j-1) b_{m,n,k} + p_{n,k,j} e^{im\theta_j} \right) / j \,. \tag{18}$$

Herein θ_j is the azimuthal angle of the rake. This is basically a phase locked averaging process, which filters off the broadband noise. Azimuthal modes are measured at *K* radial positions r_k. Amplitudes of radial modes are calculated by projection:

$$a_{m\mu,n} = \sum_{k=1}^{K} b_{m,n,k} r_k G_{m\mu}(r_k) \Bigg/ \sum_{k=1}^{K} r_k G_{m\mu}(r_k)^2 \,. \tag{19}$$

C. Breakdown into upstream and downstream propagation

Radial mode amplitudes are calculated at two axial positions: x_1 and x_2. This enables the breakdown into a downstream and an upstream propagating part:

$$a_{m\mu,n}(x) = A^{+}_{m\mu,n} \exp\left(i\alpha^{+}_{m\mu,n} x \right) + A^{-}_{m\mu,n} \exp\left(i\alpha^{-}_{m\mu,n} x \right). \tag{20}$$

Herein we have

$$\begin{cases} \alpha^{+}_{m\mu,n} = \left(M\omega_n - \xi_{m\mu}(\omega_n) \right) / \beta^2 \,, \\ \alpha^{-}_{m\mu,n} = \left(M\omega_n + \xi_{m\mu}(\omega_n) \right) / \beta^2 \,, \end{cases} \tag{21}$$

with

$$\omega_n = n\Omega \,, \tag{22}$$

where Ω is the (non-dimensional) angular frequency of the shaft. We can solve $A^{+}_{m\mu,n}$ and $A^{-}_{m\mu,n}$ from the following system of equations

$$\begin{cases} A^{+}_{m\mu,n} \exp\left(i\alpha^{+}_{m\mu,n}x_1\right) + A^{-}_{m\mu,n} \exp\left(i\alpha^{-}_{m\mu,n}x_1\right) = a_{m\mu,n}(x_1), \\ A^{+}_{m\mu,n} \exp\left(i\alpha^{+}_{m\mu,n}x_2\right) + A^{-}_{m\mu,n} \exp\left(i\alpha^{-}_{m\mu,n}x_2\right) = a_{m\mu,n}(x_2). \end{cases} \tag{23}$$

The solution is

$$\begin{cases} A^{+}_{m\mu,n} = \dfrac{1}{Q_{m\mu,n}}\left(\exp\left(i\alpha^{-}_{m\mu,n}x_2\right)a_{m\mu,n}(x_1) - \exp\left(i\alpha^{-}_{m\mu,n}x_1\right)a_{m\mu,n}(x_2)\right), \\ A^{-}_{m\mu,n} = \dfrac{1}{Q_{m\mu,n}}\left(-\exp\left(i\alpha^{+}_{m\mu,n}x_2\right)a_{m\mu,n}(x_1) + \exp\left(i\alpha^{+}_{m\mu,n}x_1\right)a_{m\mu,n}(x_2)\right), \end{cases} \tag{24}$$

with

$$Q_{m\mu,n} = 2i\exp\left(\frac{i(x_1+x_2)}{\beta^2}M\omega_n\right)\sin\left(\frac{\Delta x}{\beta^2}\xi_{m\mu}(\omega_n)\right). \tag{25}$$

D. Breakdown limitation

The denominator $Q_{m\mu,n}$ in (24) needs to be non-zero. A sufficient condition is

$$\frac{\Delta x}{\beta^2}\xi_{m\mu}(\omega) < \pi \,. \tag{26}$$

For fixed frequency, the largest value for the left hand side is found for plane waves $(m,\mu)=(0,1)$, when $\xi_{m\mu}(\omega)=\omega$. Therefore, Eq. (26) reduces to the following condition:

$$\frac{\Delta x}{\beta^2}\omega < \pi \,. \tag{27}$$

Thus, a breakdown into upstream and downstream propagating modes is possible for frequencies satisfying

$$\frac{\omega}{\beta} < \frac{\pi\beta}{\Delta x} \approx 92.4\beta \,. \tag{28}$$

This includes the major part of the frequency range mentioned in Section III.C.

V. Error analysis

For a number of reasons, inaccuracies are possible in the results of the mode detection analysis described in the previous section. For a particular mode (fixed frequency and mode order), errors may be made in the detected level and scattering may occur to other frequencies and/or mode orders. Some causes of errors are directly related to the rotation of the rake, others are more generic. A discussion of the impact follows hereafter.

A. The effect of rake rotation

Suppose that an acoustic mode exists with engine order n_0 and azimuthal order m_0:

$$p(\theta,t) = \exp\left[i\left(n_0\Omega t - m_0\theta\right)\right]. \tag{29}$$

Since the rake is moving, the pressure measured by a transducer on the rake is

$$s_k(t) = \exp\left[i\left(n_0\Omega t - m_0\theta(t)\right)\right]. \tag{30}$$

The Fourier transform follows from (14), where we can set

$$t_j = -\pi/\Omega,\; t_{j+1} = \pi/\Omega,\; \theta(t) = \theta_j + \psi t \,, \tag{31}$$

in which ψ is the angular speed of the rake. The result is

$$p_{k,j,n} = 2(-1)^{n_0} \exp\left[-im_0\theta_j\right] \frac{\sin\left(\pi m_0 \psi/\Omega\right)}{\pi\left[m_0 \psi/\Omega - \left(n_0 - n\right)\right]}. \tag{32}$$

Hence, for $n = n_0$ the rake rotation induces a reduction in amplitude, by a factor

$$\frac{\sin\left(\pi m_0 \psi/\Omega\right)}{\pi m_0 \psi/\Omega} \approx 1 - \frac{1}{6}\left(\pi m_0 \psi/\Omega\right)^2. \tag{33}$$

Furthermore, for $n \neq n_0$ frequency scattering (Doppler shift) occurs by a factor

$$\frac{\sin\left(\pi m_0 \psi/\Omega\right)}{\pi\left[m_0 \psi/\Omega - \left(n_0 - n\right)\right]} \approx \frac{m_0 \psi/\Omega}{n - n_0}. \tag{34}$$

Maximum scatter occurs for $n - n_0 = 1$ and $m_0 = 95$. Compared to the sound pressure level at engine order n_0 the maximum scattered level is $20\log(95\psi/\Omega)$ dB. The ratio ψ/Ω is always less than 10^{-4}. Hence, the maximum level reduction is 0.001 dB, and the level of the scattered frequency is at least 40 dB below the level of the input frequency. Thus, it is justified to neglect the effects of rake rotation, unlike NASA's rotating rake device[7,8].

B. Tolerance in the rake position

Obviously, the moving position of the rake needs to be tracked as accurately as possible. Mode detection errors due to errors made in the rake position can be quantified as follows.

Consider an acoustic mode with azimuthal order m_0. Suppose δ_j is the random error made in the rake position θ_j. Then the following azimuthal modes will be detected:

$$b_m = \frac{1}{J}\sum_{j=1}^{J} \exp\left[i\left(m - m_0\right)\theta_j\right] \exp\left(-im_0\delta_j\right), \tag{35}$$

where J is the total number of shaft revolutions during acquisition time. It is assumed that $m_0\delta_j$ is small, so that we can truncate the Taylor series expansion of the "exp" function. This gives us

$$b_m = \frac{1}{J}\sum_{j=1}^{J} \exp\left[i\left(m - m_0\right)\theta_j\right]\left(1 - im_0\delta_j\right). \tag{36}$$

For $m \neq m_0$ we have

$$b_m = -\frac{im_0}{J}\sum_{j=1}^{J} \exp\left[i\left(m - m_0\right)\theta_j\right]\delta_j. \tag{37}$$

The expectation value of $|b_m|^2$ is

$$E\left\{|b_m|^2\right\} = \frac{m_0^2}{J^2}\sum_{j=1}^{J} E\left\{\delta_j^2\right\} = \frac{m_0^2\sigma^2}{J}, \tag{38}$$

where σ is the standard deviation of the rake position error.

In the present set-up, it was found that the standard deviation is not more than 0.1°. Further, during 10 minutes of acquisition time, there are at least $J = 10000$ shaft revolutions. Thus (with $m_0 = 95$), the mode scatter level is at most −55 dB.

For $m = m_0$ we may expect some reduction in mode amplitude level. To estimate this, we expand the Taylor series of the "exp" function in (35) up to the second order:

$$b_m = \frac{1}{J}\sum_{j=1}^{J} \exp\left(-im_0\delta_j\right) \approx \frac{1}{J}\sum_{j=1}^{J}\left(1 - im_0\delta_j - \frac{1}{2}m_0^2\delta_j^2\right). \tag{39}$$

Herewith we obtain

$$E\left\{b_m\right\} = 1 - \frac{1}{2}m_0^2\sigma^2, \tag{40}$$

which is not more than 0.12 dB.

C. The effect of uncovered rake angles

Another limitation of this rake is that it does not cover the full range of azimuthal angles, as there is an uncovered range of 4°. This may cause aliasing of modes. To quantify this, let us assume the presence of an azimuthal mode

$$p(\theta) = \exp\left(-im_0\theta\right). \tag{41}$$

If the rake rotates from $\theta = \theta_1$ to $\theta = \theta_2$, it will detect the following mode amplitudes:

$$b_m = \frac{1}{\theta_2 - \theta_1} \int_{\theta_1}^{\theta_2} p(\theta) \exp\left(im\theta\right) d\theta = \frac{1}{\theta_2 - \theta_1} \int_{\theta_1}^{\theta_2} \exp\left[i(m - m_0)\theta\right] d\theta. \tag{42}$$

For $m = m_0$ we find the correct value: $b_m = 1$. However, for $m \neq m_0$ we find

$$b_m = \frac{\exp\left[i(m - m_0)\theta_2\right] - \exp\left[i(m - m_0)\theta_1\right]}{i(m - m_0)\left(\theta_2 - \theta_1\right)}, \tag{43}$$

where the correct value is $b_m = 0$. Hence, spurious (scattered) modes will be detected.

The maximum scattered level if obtained for $m - m_0 = \pm 1$. With $\theta_1 = \pi/90$ (2°) and $\theta_2 = 2\pi - \pi/90$ (358°) this is 0.0112, in other words, 39 dB below the level of the actual mode.

D. Radial mode scattering

The algorithm to determine the radial mode is given by Eq. (19). Just like the azimuthal modes, any input radial mode will be detected at the correct amplitude, but other (scattered) modes will be "detected" as well, at much lower levels. These levels depend on the azimuthal mode number, on the input radial mode number, and on the scattered mode number. A numerical survey showed that the scattered mode levels stay at least 56 dB below the actual mode level.

E. Accuracy of pulse time determination

Suppose that γ_j is the random error made in the length of the pulse interval $t_{j+1} - t_j$. Then we have for the assumed angular shaft speed:

$$\Omega_a = \frac{2\pi}{t_{j+1} - t_j + \gamma_j} = \frac{2\pi}{t_{j+1} - t_j} \times \frac{1}{1 + \dfrac{\gamma_j}{t_{j+1} - t_j}} \approx \frac{2\pi}{t_{j+1} - t_j}\left(1 - \frac{\gamma_j}{t_{j+1} - t_j}\right) = \Omega\left(1 - \frac{\Omega\gamma_j}{2\pi}\right). \tag{44}$$

With input sound at engine order n_0, the following output engine orders will be detected:

$$\begin{aligned} p_{j,n} &= (-1)^n \frac{\Omega_a}{\pi} \int_{-\pi/\Omega_a}^{\pi/\Omega_a} \exp\left[i\left(n_0\Omega - n\Omega_a\right)t\right] dt \approx (-1)^n \frac{\Omega_a}{\pi} \int_{-\pi/\Omega_a}^{\pi/\Omega_a} \exp\left[i\left(n_0\Omega - n\Omega\left(1 - \frac{\Omega\gamma_j}{2\pi}\right)\right)t\right] dt \\ &= 2(-1)^n \frac{\sin\left[\dfrac{\Omega\pi}{\Omega_a}\left(n_0 - n\left(1 - \dfrac{\Omega\gamma_j}{2\pi}\right)\right)\right]}{\dfrac{\Omega\pi}{\Omega_a}\left(n_0 - n\left(1 - \dfrac{\Omega\gamma_j}{2\pi}\right)\right)} \approx 2(-1)^n \frac{\sin\left[\pi\left(n_0 - n\left(1 - \dfrac{\Omega\gamma_j}{2\pi}\right)\right)\right]}{\pi\left(n_0 - n\left(1 - \dfrac{\Omega\gamma_j}{2\pi}\right)\right)}. \end{aligned} \tag{45}$$

For $n = n_0$ we have a reduction

$$p_{j,n} \approx 2(-1)^n \frac{\sin\left(n\Omega\gamma_j/2\right)}{n\Omega\gamma_j/2} \approx 2(-1)^n \left[1 - \frac{1}{6}\left(\omega_n\gamma_j/2\right)^2\right]. \tag{46}$$

For $n \neq n_0$ we can write:

$$p_{j,n} \approx 2(-1)^{n_0} \frac{\sin\left[n\Omega\gamma_j/2\right]}{\pi\left(n_0 - n\right)} \approx 2(-1)^{n_0} \frac{\omega_n\gamma_j/2}{\pi\left(n_0 - n\right)}. \tag{47}$$

The expectation value of $\gamma_j^{\,2}$ was found to be approximately 8×10^{-6}. For $\omega_n = 100$ this corresponds to 0.03 dB reduction. The level of the scattered frequencies is at most –27 dB.

F. Error analysis summary

Scattering of mode detection data into other frequencies or into other modes occurs due to the rotation of the rake, errors made in the assumed location of the rake, the uncovered range of rake angles, the limited number of radial sensor locations, and to errors made in the pulse time determination. In the present experimental set-up, the pulse time errors cause the largest scatter levels. It is noted that these errors are not specific to a moving rake.

VI. Typical results

A. Tonal sound and broadband noise

A typical breakdown into tonal sound and broadband noise is shown in Figure 2. The spectra are averaged over all Kulites. The tonal sound of the rake Kulites was calculated by summing all cut-on modes. This figure shows that the acquisition time of 10 minutes enables a good separation. Although a number of tonal peaks protrude above the broadband noise levels, it is observed that broadband noise prevails. This broadband noise, however, is partly be due to the rake itself and the inner sleeve rotating system.

It is noted that the traditional phase locked method for obtaining tonal sound does not work for the rake Kulites, because of the motion of the rake.

B. Azimuthal modes

Typical spectra of azimuthal modes (tonal sound) at BPF are shown in Figure 3. Both spectra correspond to the same LPT configuration. The only difference is the reversed rotation of the rake, which proves that the results are independent of the rake rotation direction. The spectra feature an $m = 4$ mode, which is scattered by the 16 vanes of the TRF into modes $m = -28, -12, 20$. The levels of the cut-off modes ($|m| > 30$) are residues of broadband noise, and are therefore different for both measurements.

C. Radial modes

Figure 4 shows a typical radial mode spectrum, for fixed azimuthal mode number at BPF, split into upstream and downstream propagating part. The downstream propagating modes dominate, as expected. The modes are cut-on up to $\mu = 3$. The levels of the cut-off modes are, again, much lower than the cut-on levels and residues of broadband noise.

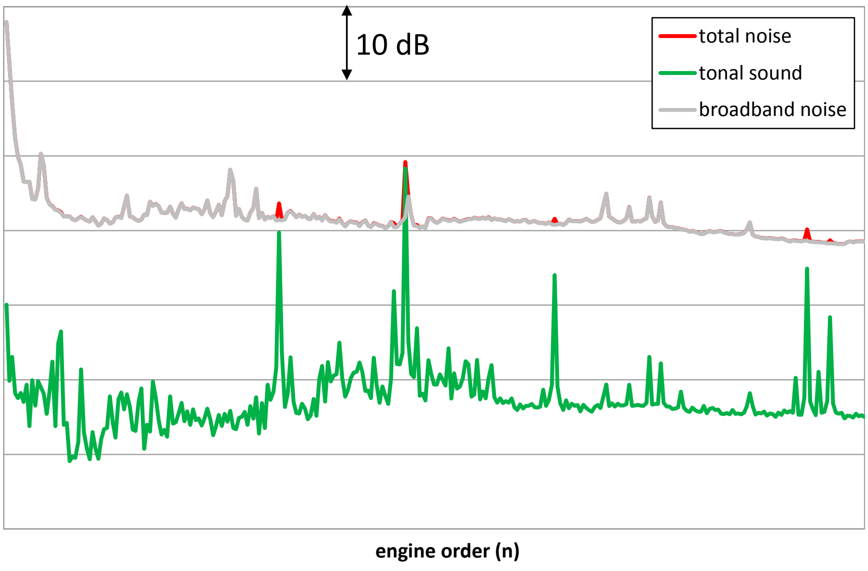

Figure 2 Breakdown into tonal and broadband noise.

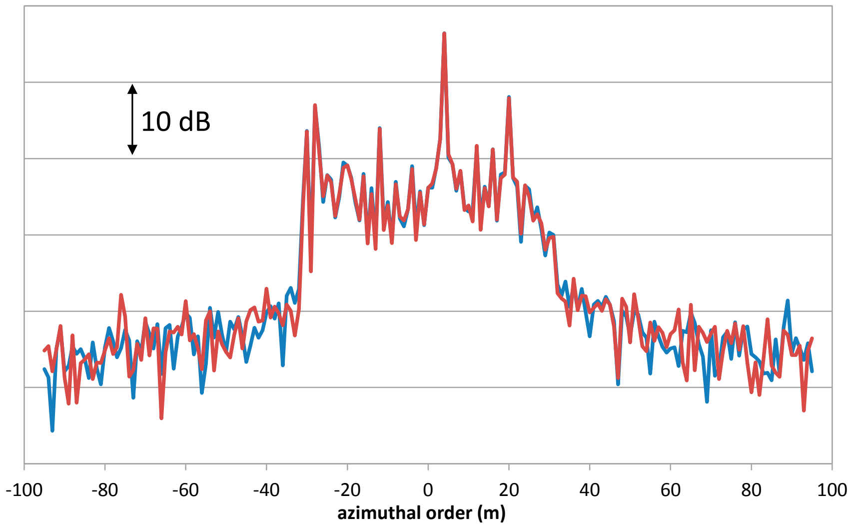

Figure 3 Typical azimuthal spectra (repeat measurements at opposite rotation directions).

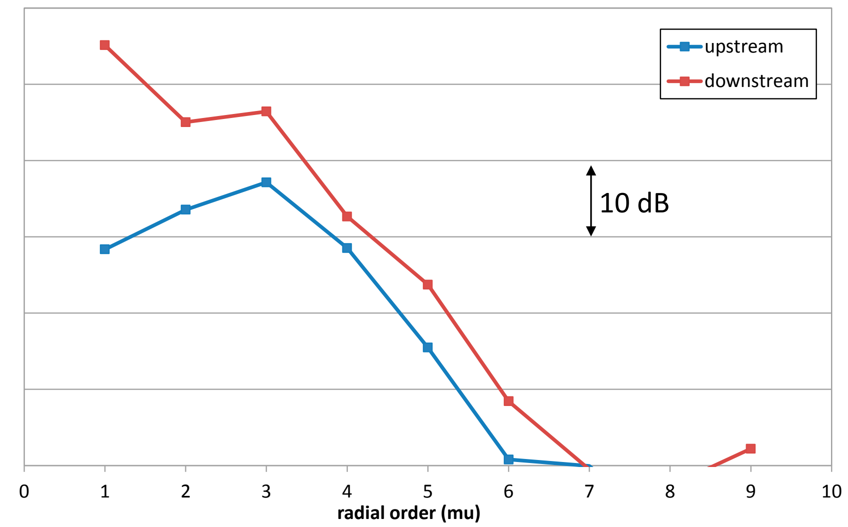

Figure 4 Typical radial mode spectrum, upstream and downstream propagating.

VII. Conclusions

A new detection device for azimuthal and radial acoustic modes in a duct downstream of an axial flow LPT was presented. The features are:

- Measurements are done with a radial rake with 10 sensor holders.
- Each holder contains 2 Kulite sensors, thus enabling separation between upstream and downstream propagating modes.
- The rake performs one rotation of 10 minutes in a slow continuous motion.

The measurement time is significantly shorter than with conventional radial mode measurements, where the rake is positioned on a large number of static angular positions. On the other hand, the rake rotation speed is much lower than the shaft speed, which rules out the need for time-consuming corrections for Doppler frequency shift. Hence, this device combines the advantages of a short acquisition time and a short post-processing time.

An error analysis showed that this new device does not suffer from loss of performance compared to other mode detection devices. The merits were demonstrated by an application to typical measurements on an LPT component.

Acknowledgments

The rake was manufactured by the “Engineering & Technical Services” department of NLR. The LPT design and the tests in the “1T” facility were led by Snecma. The acoustic measurements were arranged by Evert Geurts (NLR).

References

[1]Nesbitt, E., “Towards a Quieter Low Pressure Turbine: Design Characteristics and Prediction Needs”, *International Journal of Aeroacoustics*, Vol, 10, Nr. 1, 2011, pp. 1-16.

[2]Broszat, D., Korte, D., Tapken, U., and Moser, M., “Validation of Turbine Noise Prediction Tools with Acoustic Rig Measurements”, AIAA Paper 2009-3283, May 2009.

[3]Rademaker, E.R., Sijtsma, P., and Tester, B.J., “Mode Detection with an Optimised Array in a Model Turbofan Engine Intake at Varying Shaft Speeds,” AIAA Paper 2001-2181, May 2001.

[4]Tyler, J.M. and Sofrin, T.G., “Axial Flow Compressor Noise Studies”, *SAE Transactions*, Vol. 70, pp. 309-332, 1962.

[5]Enghardt, L., Tapken, U., Neise, W., Kennepohl, F., and Heinig, K., “Turbine Blade/Vane Interaction Noise: Acoustic Mode Analysis Using In-Duct Sensor Rakes”, AIAA Paper 2001-2153, May 2001.

[6]Tapken, U., Bauers, R., Neuhaus, L., Humphreys, N., Wilson, A., Stöhr, C., and Beutke, M., “A New Modular Fan Rig Noise Test and Radial Mode Detection Capability”, AIAA Paper 2011-2897, June 2011.

[7]Heidelberg, L., and Hall, D., “Inlet Acoustic Mode Measurements Using a Continously Rotating Rake”, *AIAA Journal of Aircraft*, Vol. 32, 1995, pp. 761-767.

[8]Sutliff, D., Rotating Rake Turbofan Duct Mode Measurement System, NASA TM 2005-213828, 2005.